CHAPTER 4

# THERMAL DIFFUSION AND HEAT GENERATION EFFECTS ON ONE DIMENSIONAL MHD NANOFLUID FLOW

Content of this chapter is published in Journal of Molecular Liquids (Elsevier), 257 (2018) 12-25.

# Chapter 4

## THERMAL DIFFUSION AND HEAT GENERATION EFFECTS ON ONE DIMENSIONAL MHD NANOFLUID FLOW

In nuclear enrichment, thermal power generation and many large scale industries involving liquid metals, knowledge of effects of heat generation and thermal diffusion is essential. Present investigation involves study of thermal diffusion and heat generation effects on unsteady magnetohydrodynamics flow of radiating and electrically conducting nanofluid past over an oscillating vertical plate through porous medium.

## 4.1 Introduction of the Problem

Heat generation is evident in numerous significant processes such as storage of radioactive supplies, reactor safety and byproducts of consumed nuclear fuel. Das et al. [10] investigated nanofluid flow of non-uniform heat generation/absorption. Study of Soret effect or Thermo-diffusion is important in groundwater contaminant movement, solidification of alloys, oil-reservoirs and chemical reactors. Nadeem et al. [48] discussed Thermo-diffusion effects on MHD nanofluid flow. Heat transfer in porous media has several uses such as geophysical processes, geothermal reservoirs, nuclear waste dumping and chemical reactor. Thus, coupled study of heat generation/absorption effects, thermal diffusion and heat transfer in nanofluid flow is significant in processes related to Uranium enrichment and nuclear reactors. Keeping this in view, investigations of previous chapters are extended taking heat generation and Soret effect into consideration.

## 4.2 Novelty of the Problem

Effects of thermal diffusion and heat generation on the unsteady natural convective magnetohydrodynamics flow of radiating and electrically conducting nanofluid past over an oscillating vertical plate embedded in porous medium are analyzed.

## 4.3 Formulation of the problem

As shown in Figure 4.1, nanofluid flow is observed in positive $y'$ direction (i.e. normal to the plate) in presence of uniform magnetic field $B$.

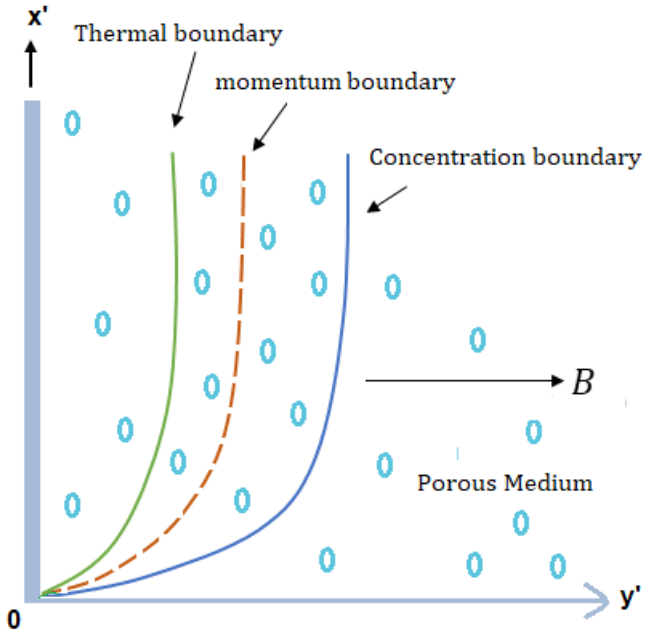


**Figure 4.1:** Physical sketch of the problem

It is assumed that, initially temperature of both, fluid and the plate is $T_0$ and concentration near the plate is $C_0$. At time $t' > 0$, temperature is considered to be $T_0 + (T_w - T_0)\, {t'}/{t_0}$ when time $t' \leq t_0$ and $T_w$ when $t' > t_0$. Concentration is assumed to be $C_0 + (C_w - C_0)\, {t'}/{t_0}$ when time $t' \leq t_0$, $C_w$ when $t' > t_0$. Oscillations of the plate is governed by $u' = u_0 \cos(\omega' t')$, where $\omega'$ is the frequency of oscillation of the plate.

Under above conventions; momentum, energy and mass transfer equations can be expressed as

$$\rho_{nf}\frac{\partial u'}{\partial t'} = \mu_{nf}\frac{\partial^2 u'}{\partial y'^2} - \sigma_{nf}B^2 u' - \frac{\mu_{nf}\varphi}{k_1}u' + g(\rho\beta)_{nf}(T' - T_0) + g(\rho\beta_C)_{nf}(C' - C_0), \quad (4.1)$$

$$\frac{\partial T'}{\partial t'} = \frac{k_{nf}}{(\rho c_p)_{nf}}\frac{\partial^2 T'}{\partial y'^2} + \frac{Q(T' - T_0)}{(\rho c_p)_{nf}}, \quad (4.2)$$

$$\frac{\partial C\prime}{\partial t'} = D_C \frac{\partial^2 C\prime}{\partial y\prime^2} + D_T \frac{\partial^2 T'}{\partial y\prime^2} - k'(C' - C_0), \tag{4.3}$$

where

$$\rho_{nf} = (1 - \emptyset)\rho_f + \emptyset\rho_s, \tag{4.4}$$

$$\mu_{nf} = \frac{\mu_f}{(1-\emptyset)^{2.5}}, \tag{4.5}$$

$$\sigma_{nf} = \sigma_f \left[1 + \frac{3(\sigma-1)\emptyset}{(\sigma+2)-(\sigma-1)\emptyset}\right], \tag{4.6}$$

$$\sigma = \frac{\sigma_s}{\sigma_f}, \tag{4.7}$$

$$(\rho\beta)_{nf} = (1 - \emptyset)(\rho\beta)_f + \emptyset(\rho\beta)_s, \tag{4.8}$$

$$k_{nf} = k_f \left[1 - 3\frac{\emptyset(k_f - k_s)}{2k_f + k_s + \emptyset(k_f - k_s)}\right], \tag{4.9}$$

$$\left(\rho c_p\right)_{nf} = (1 - \emptyset)(\rho c_p)_f + \emptyset(\rho c_p)_s, \tag{4.10}$$

with boundary conditions

$$u' = 0, \quad T' = T_0, \ \ C' = C_0; \ as \ \ y' \geq 0 \ and \ \ t' = 0; \tag{4.11}$$

$$u' = u_0 \cos(\omega' t'),$$

$$T' = \begin{cases} T_0 + (T_w - T_0)\, {t'}/{t_0} & if \ \ 0 < t' < t_0 \\ T_w & if \quad t' \geq t_0 \end{cases},$$

$$C' = \begin{cases} C_0 + (C_w - C_0)\, {t'}/{t_0} & if \ \ 0 < t' < t_0 \\ C_w & if \quad t' \geq t_0 \end{cases}, \ \ as \ \ t' \geq 0 \ and \ y' = 0; \tag{4.12}$$

$$u' \to 0, T' \to T_0, \ \ C' \to C_0; \ as \ \ y' \to \infty \ and \ t' \geq 0. \tag{4.13}$$

Introducing non dimensional variables

$$y = \frac{u_0 y\prime}{v_f}, t = \frac{{u_0}^2 t'}{v_f}, u = \frac{u'}{u_0}, \theta = \frac{T' - T_0}{T_w - T_0}, \omega = \frac{v_f \omega'}{{u_0}^2}, \ \ C = \frac{C\prime - C_0}{C_w - C_0}, \tag{4.14}$$

System becomes:

$$\frac{\partial u}{\partial t} = a_1 \frac{\partial^2 u}{\partial y^2} - \left(a_3 M + \frac{a_1}{k}\right) u + a_2 G_r \theta + G_m a_5 C, \tag{4.15}$$

$$\frac{\partial \theta}{\partial t} = a_4 \frac{\partial^2 \theta}{\partial y^2} + H\theta, \tag{4.16}$$

$$\frac{\partial C}{\partial t} = \frac{1}{s_c}\frac{\partial^2 C}{\partial y^2} + Sr\frac{\partial^2 \theta}{\partial y^2} - R_\gamma C, \tag{4.17}$$

with initial and boundary conditions

$$u = 0, \quad T = T_0, \ C = C_0; \ as \ y \geq 0 \ and \ t = 0; \tag{4.18}$$

$u = \cos(\omega t)$ ,

$$\theta = \begin{cases} t, & 0 < t \leq 1 \\ 1 & t > 1 \end{cases} = tH(t) - (t-1)H(t-1),$$

$$C = \begin{cases} t, & 0 < t \leq 1 \\ 1 & t > 1 \end{cases} = tH(t) - (t-1)H(t-1), \ y = 0, \ t > 0; \tag{4.19}$$

$$u \to 0, \theta \to 0, C \to 0 \quad as \ y \to \infty, t > 0; \tag{4.20}$$

where

H (.) is Heaviside unit step function,

$$b_0 = 1 - \emptyset, \tag{4.21}$$

$$b_1 = (b_0 + \emptyset\frac{\rho_s}{\rho_f}), \tag{4.22}$$

$$b_2 = (b_0 + \emptyset\frac{(\rho\beta)_s}{(\rho\beta)_f}), \tag{4.23}$$

$$b_3 = (b_0 + \emptyset\frac{(\rho c_p)_s}{(\rho c_p)_f}), \tag{4.24}$$

$$b_4 = \frac{k_{nf}}{k_f}, \tag{4.25}$$

$$b_5 = \frac{\sigma_{nf}}{\sigma_f}, \tag{4.26}$$

$$b_6 = \frac{b_4}{b_3}, \tag{4.27}$$

$$b_7 = (b_0 + \emptyset \frac{(\rho\beta)_c}{(\rho\beta)_f}), \quad (4.28)$$

$$a_1 = \frac{1}{{b_0}^{2.5} b_1}, \quad (4.29)$$

$$a_2 = \frac{b_2}{b_1}, \quad (4.30)$$

$$a_3 = \frac{b_5}{b_1}, \quad (4.31)$$

$$a_4 = \frac{b_6}{pr}, \quad (4.32)$$

$$a_5 = \frac{b_7}{b_1}, \quad (4.33)$$

$$H = a_1 b_6, \quad (4.34)$$

$$Pr = \frac{\mu_f \left(\rho c_p\right)_f}{\rho_f k_f}, \quad (4.35)$$

$$M = \frac{\sigma_f B^2 v_f}{\rho_f {u_0}^2}, \quad (4.36)$$

$$\frac{1}{k} = \frac{v_f \varphi^2}{k_1 {u_0}^2}, \quad (4.37)$$

$$Gr = \frac{g\beta_f (T_w - T_0) v_f}{{u_0}^3}, \quad (4.38)$$

$$Sc = \frac{v_f}{D_C}, \quad (4.39)$$

$$Sr = \frac{D_T (T_w - T_0)}{v_f (C_w - C_0)}, \quad (4.40)$$

$$R_\gamma = \frac{v_f k'}{{u_0}^2}, \quad (4.41)$$

$$Gm = \frac{g\beta_c v_f (C_w - C_0)}{{u_0}^3}. \quad (4.42)$$

## 4.4 Solution of the problem

Solutions for the system is derived in a similar way as in previous chapters.

### 4.4.1 For ramped wall temperature and ramped surface concentration

The solution of the problem for ramped wall temperature and ramped surface concentration is derived by solving equations (4.15) to (4.17) with initial and boundary conditions (4.18) to (4.20) and is given by

$$\theta(y,t) = f_9(y,t) - f_9(y,t-1)H(t-1), \tag{4.43}$$

$$C(y,t) = h_2(y,t) - h_2(y,t-1)H(t-1), \tag{4.44}$$

$$u(y,t) = g_1(y,t) + h_1(y,t) - h_1(y,t-1)H(t-1). \tag{4.45}$$

### 4.4.2 For isothermal temperature and ramped surface concentration

Here equations will be same except formula of $\theta$ in (4.19), which will be $\theta = 1\ at\ y = 0$, $t \geq 0$. The solution of the problem in this case is derived by solving equations (4.15) to (4.17) with new initial and boundary conditions. The solution is

$$\theta(y,t) = f_8(y,t), \tag{4.46}$$

$$C(y,t) = f_{13}(y,t) - f_{13}(y,t-1)H(t-1) + g_{12}(y,t) - g_{13}(y,t), \tag{4.47}$$

$$u(y,t) = g_1(y,t) + g_5(y,t) + g_6(y,t) - g_6(y,t-1)H(t-1) + g_7(y,t) - g_8(y,t) + g_8(y,t-1)H(t-1) - g_9(y,t). \tag{4.48}$$

### 4.4.3 For isothermal temperature and constant concentration

Here equations will be same except formula of $\theta$ and $C$ in equation (4.19) that becomes

$C = 1, \theta = 1\ at\ y = 0, t \geq 0$. The solution of the problem in this case is derived by solving equations (4.15) to (4.17) with new initial and boundary conditions. The solution is

$$\theta(y,t) = f_8(y,t) \tag{4.49}$$

$$C(y,t) = f_{12}(y,t) + g_{12}(y,t) - g_{13}(y,t) \tag{4.50}$$

$$u(y,t) = h_3(y,t) \tag{4.51}$$

Expressions of Nusselt number Nu, Sherwood Number Sh and Skin friction $C_f$ for all three cases, are calculated from equations (4.43) to (4.48),

## 4.5 Nusselt Number:

### 4.5.1 For ramped wall temperature and ramped surface concentration

$$Nu = -[J_9(t) - J_9(t-1)H(t-1)]. \tag{4.52}$$

### 4.5.2 For isothermal temperature and ramped surface concentration

$$Nu = -[J_8(t)]. \tag{4.53}$$

### 4.5.3 For isothermal temperature and constant concentration

$$Nu = -[J_8(t)] \tag{4.54}$$

## 4.6 Sherwood Number:

### 4.6.1 For ramped wall temperature and ramped surface concentration

$$Sh = -[J_{32}(t) - J_{32}(t-1)H(t-1)]. \tag{4.55}$$

### 4.6.2 For isothermal temperature and ramped surface concentration

$$Sh = -[J_{13}(t) - J_{13}(t-1)H(t-1) + J_{27}(t) - J_{28}(t)]. \tag{4.56}$$

### 4.6.3 For isothermal temperature and constant concentration

$$Sh = -[J_{12}(t) + J_{27}(t) - J_{28}(t)] \tag{4.57}$$

## 4.7 Skin friction:

### 4.7.1 For ramped wall temperature and ramped surface concentration

$$C_f = J_{16}(t) + J_{31}(t) - J_{31}(t-1)H(t-1). \tag{4.58}$$

### 4.7.2 For isothermal temperature and ramped surface concentration

$$C_f = J_{16}(t) + J_{20}(t) + J_{21}(t) - J_{21}(t-1)H(t-1) + J_{22}(t) - J_{23}(t) + J_{23}(t-1) * H(t-1) - J_{24}(t). \tag{4.59}$$

### 4.7.3 For isothermal temperature and constant concentration

$$C_f = J_{33}(t) \tag{4.60}$$

## 4.8 Results and Discussion

To understand the physics of the problem, the obtained analytical solutions are studied numerically and are explained with the help of graphs. Parametric study is performed for volume fraction parameter $\phi$, permeability of porous medium $\kappa$, Soret number $Sr$, Heat generation Parameter $H$ and magnetic parameter $M$ from Figure 4.2 to Figure 4.9. Numerical values of skin-friction $C_f$, Nusselt number $Nu$ and Sherwood number $Sh$ are computed and presented in tables. Figure 4.2 displays the effect of volume fraction of nanoparticles on nanofluid velocity. The nanofluid velocity increases as volume fraction parameter decreases. Since adding the particles leads to increase in dynamic viscosity and momentum diffusion of the fluid, it is clear that the thickness of the boundary layer decreases with increase in $\phi$. Figure 4.3 exhibits temperature profile for different values of volume fraction of nanoparticles, when other parameters are fixed. It is observed that velocity of the nanofluid increases with increasing volume fraction of nanoparticles.

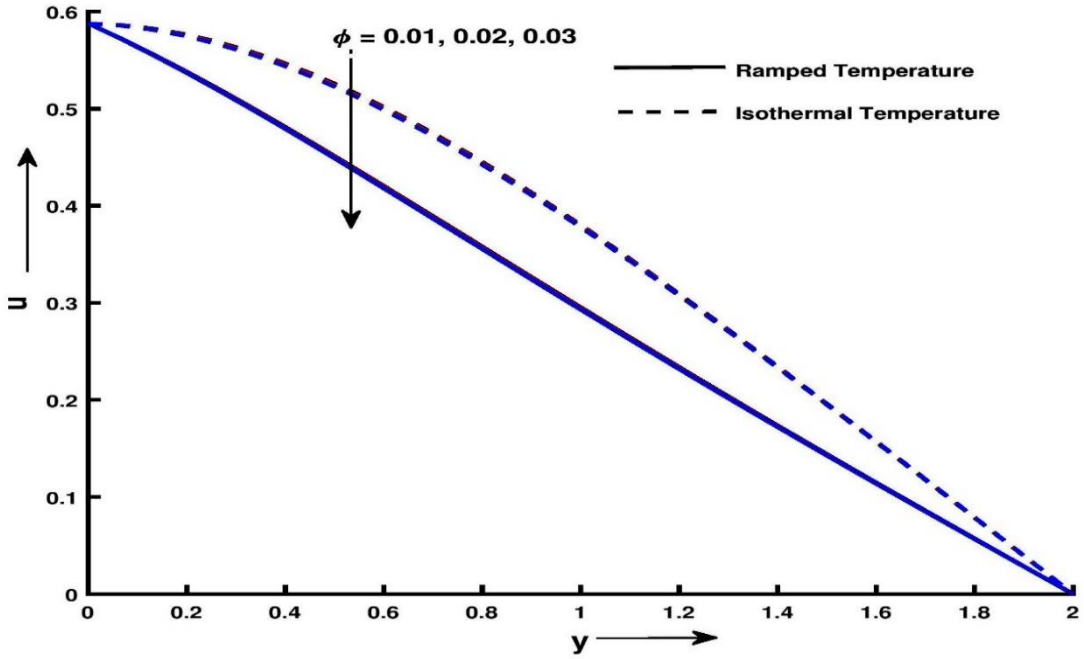


**Figure 4.2:** Velocity profile $u$ for $y$ and $\emptyset$ at $\kappa = 0.4, \mathrm{Sc} = 0.22, \mathrm{Gm} = 10,$ $Gr = 5, Sr = 15, R_\gamma = 10, Nr = 5, H = 10$ and $t = 0.4$

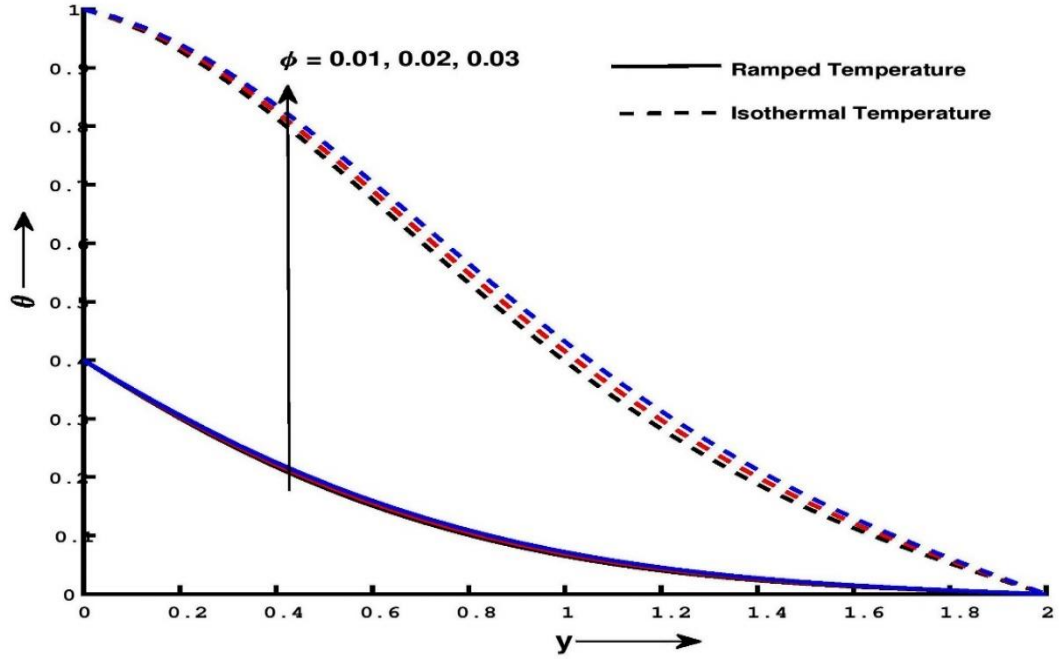


**Figure 4.3:** Temperature profile θ for $y$ and $\emptyset$ at $\kappa = 0.4, Sc = 0.22, Gm = 10,$ $Gr = 5, Sr = 15, R_\gamma = 10, Nr = 5, H = 10$ and $t = 0.4$

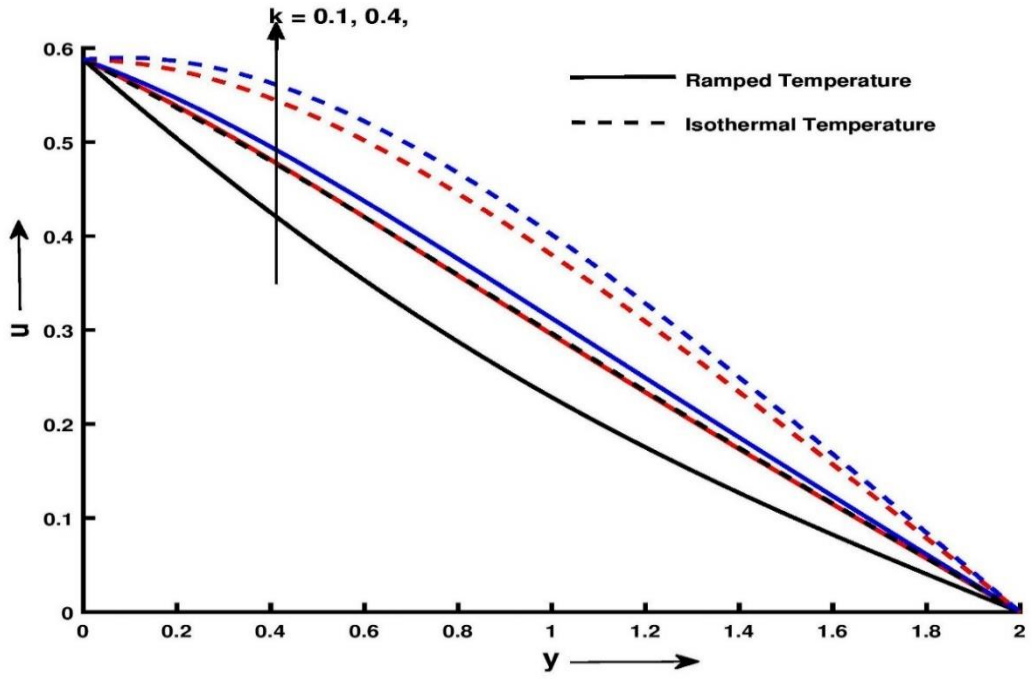


**Figure 4.4:** Velocity profile $u$ for $y$ and $\kappa$ at $\emptyset = 0.01, Sc = 0.22,\ Gm = 10,$ $Gr = 5, Sr = 15, R_\gamma = 10, Nr = 5, H = 10$ and $t = 0.4$

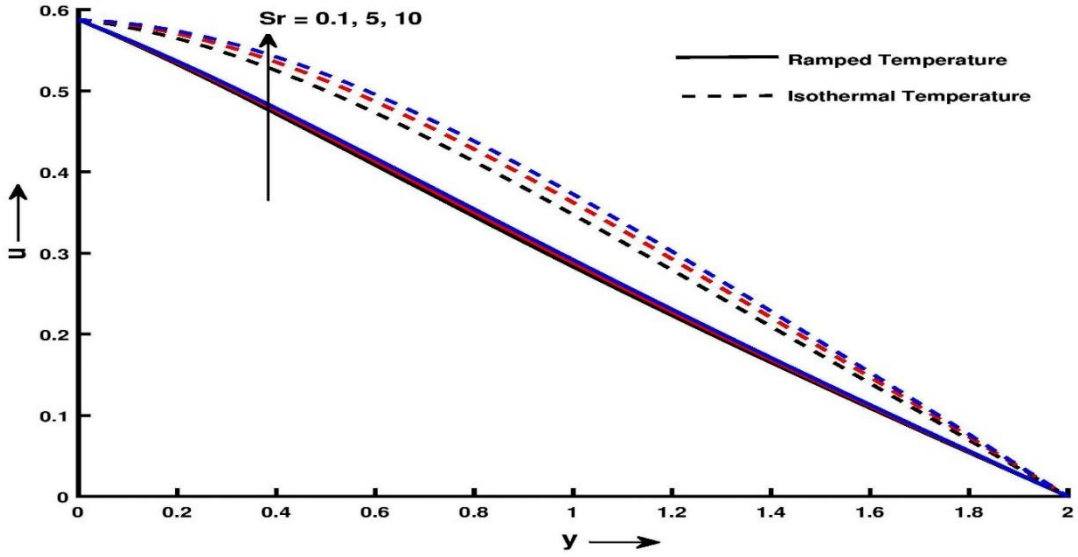


**Figure 4.5:** Velocity profile $u$ for $y$ and $Sr$ at $\emptyset = 0.01, \kappa = 0.4, Sc = 0.22,$ $Gm = 10, Gr = 5, R_\gamma = 10, Nr = 5, H = 10$ and $t = 0.4$

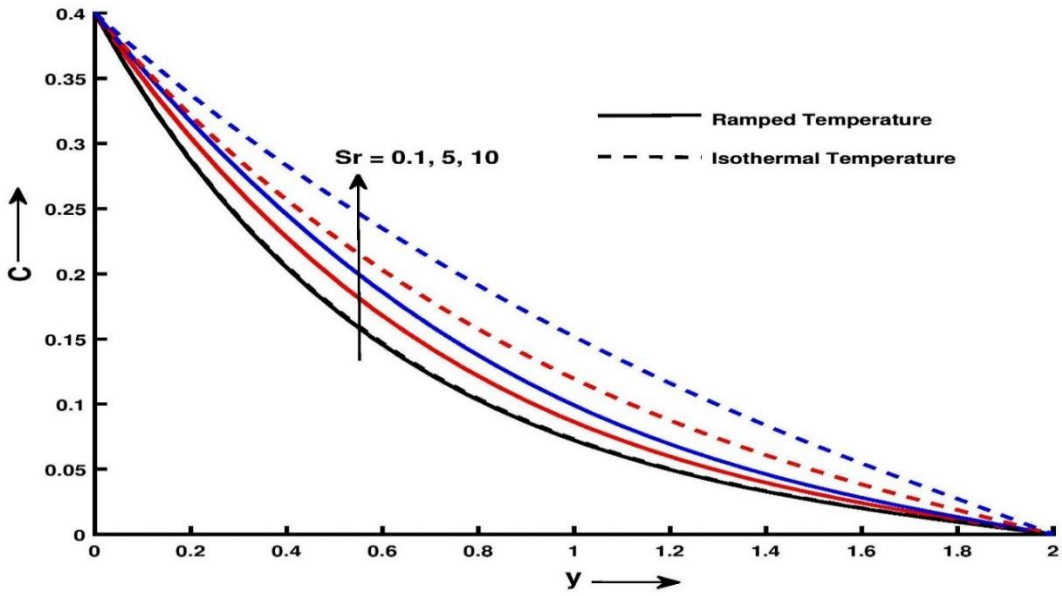


**Figure 4.6:** Concentration profile $C$ for $y$ and $Sr$ at $\emptyset = 0.01, \kappa = 0.4, Sc = 0.22,$ $Gm = 10, Gr = 5, R_\gamma = 10, Nr = 5, H = 10$ and $t = 0.4$

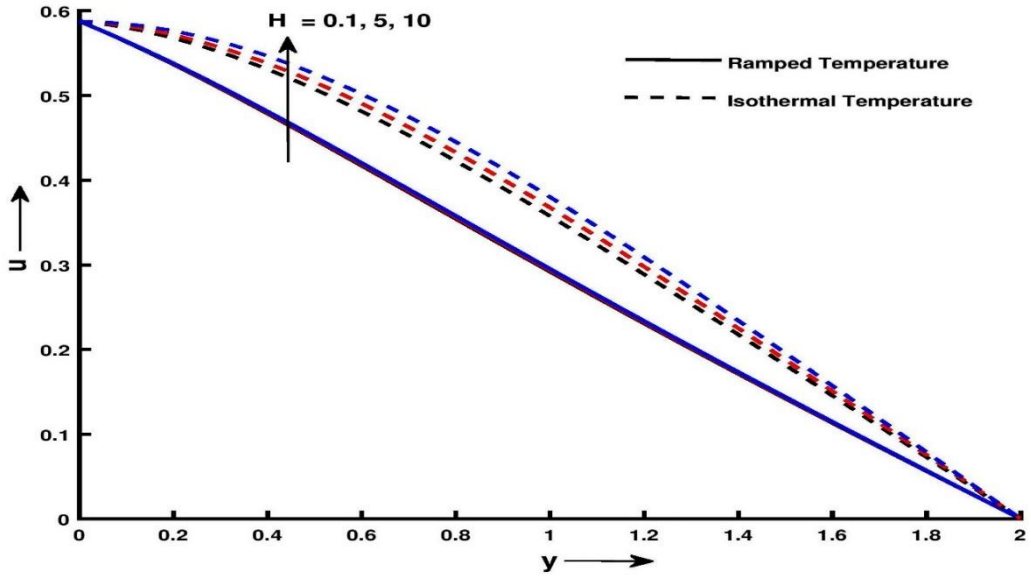


**Figure 4.7:** Velocity profile u for y and $H$ at $\emptyset = 0.01, \kappa = 0.4, Sc = 0.22,$ $Gm = 10, Gr = 5, Sr = 15, R_\gamma = 10, Nr = 5 \; and \; t = 0.4$

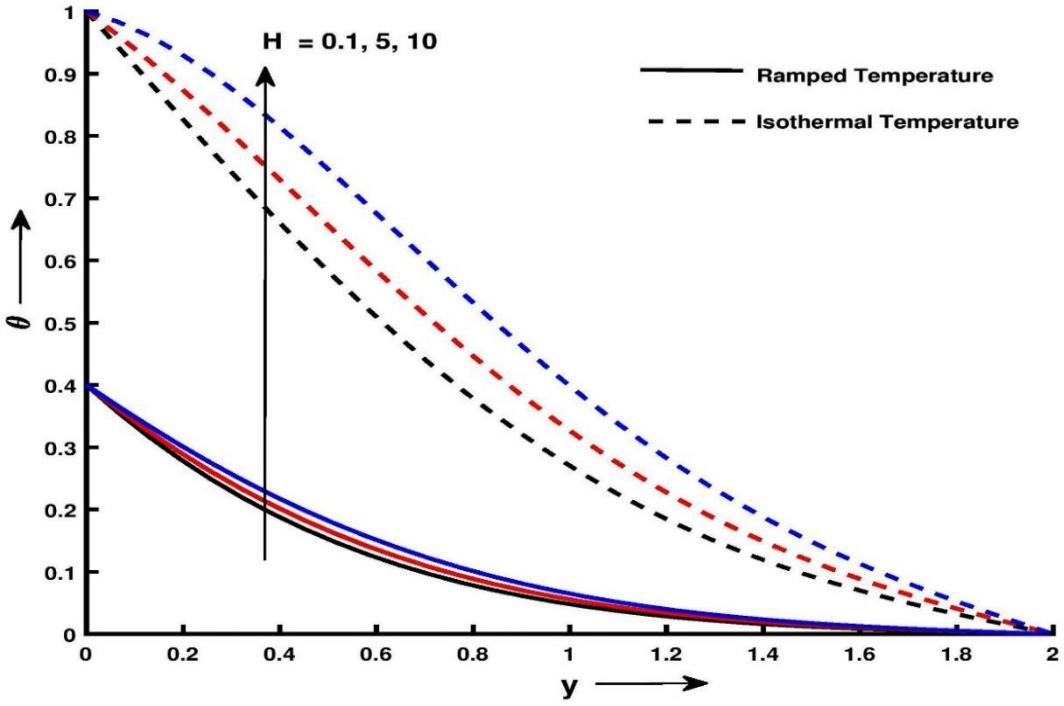


**Figure 4.8:** Temperature profile θ for $y$ and $H$ at $\emptyset = 0.01, \kappa = 0.4, Sc = 0.22,$ $Gm = 10, Gr = 5, Sr = 15, R_\gamma = 10, Nr = 5$ and $t = 0.4$

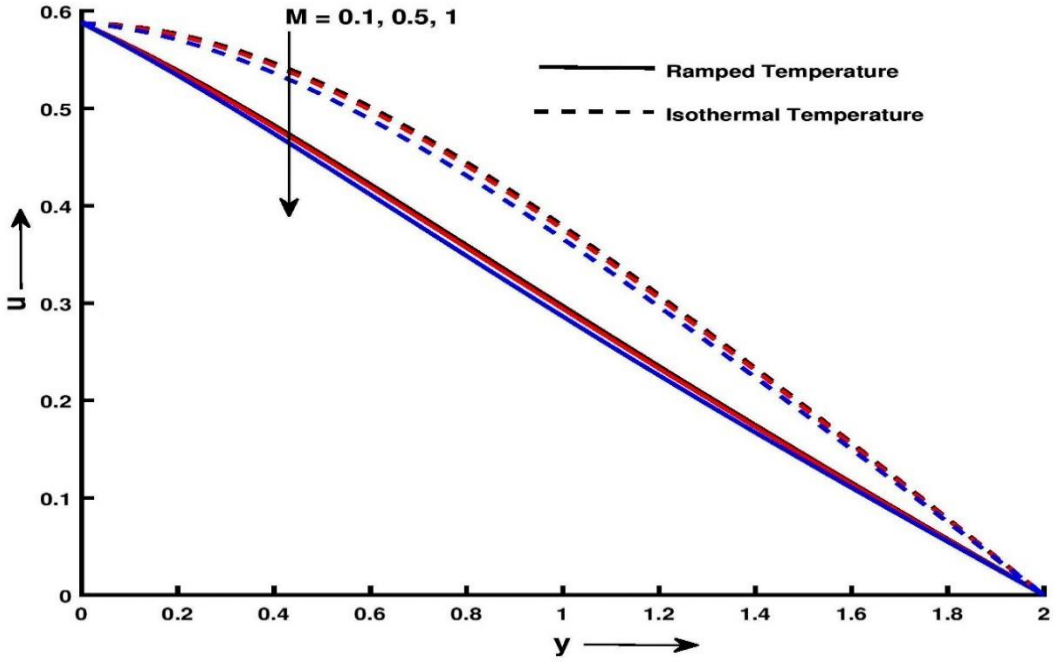


**Figure 4.9:** Velocity profile $u$ for $y$ and $M$ at $Pr = 6.2, \kappa = 0.4, Sc = 0.22,$ $Gm = 10, Gr = 5, Sr = 15, R_\gamma = 10, Nr = 5$ and $t = 0.4$

Figure 4.4 shows velocity profile for various values of permeability parameter $\kappa$ by keeping other parameters fixed. It is found that velocity increases with increase in $\kappa$. With increase in $\kappa$, the resistance of the porous medium decreases which increases the momentum of the flow regime, ultimately enhances the velocity field. Figure 4.5 depicts the velocity profile for different values of Soret number $Sr$ in both the cases. The Soret number defines the effect of the temperature gradients inducing significant mass diffusion effects. It is noticed that an increase in Soret number results in an increase in velocity. Figure 4.6 exhibits effect of thermo-diffusion on the species concentration for both ramped temperature and isothermal plates. It is evident from Figure 4.6 that, $C$ increases on increasing $Sr$ throughout the boundary layer region. Figure 4.7 demonstrates effect of the heat generation parameter $H$ on velocity profile. It is evident that increasing values of $H$ tends to increase velocity distribution. The dimensionless temperature profile along vertical plate is shown in Figure 4.8 with variations of heat generation parameter. It is clear that temperature distribution rises in presence of heat generation. Additional energy is generated in boundary layer due to the presence of heat source. Figure 4.9 reveals that nanofluid velocity decreases for increasing values of magnetic parameter $M$. Physically, it is due to the transverse magnetic field resulting in resistive Lorentz force and upon increasing values of $M$, this drag force increases leading to the deceleration of the flow.

Values of skin friction $C_f$ are presented in Table 4.1. Skin friction tends to increase with volume fraction parameter $\emptyset$ and Grashof number $Gr$ while decreases with increase in permeability of porous medium $\kappa$, Grashof number $Gm$, heat generation / absorption parameter $H$ (Negative sign of H signifies that heat is absorbed) and Schimdt number $Sc$ in the case of isothermal temperature and ramped concentration.

**Table 4.1:** Skin friction variation

| $\emptyset$ | $Sc$ | $Gr$ | $Gm$ | $\kappa$ | $H$ | $Sr$ | $t$ | Skin friction $C_f$ for Ramped temperature and ramped concentration | Skin friction $C_f$ for isothermal temperature and ramped concentration | Skin friction $C_f$ for isothermal temperature and constant Surface concentration. |
|---|---|---|---|---|---|---|---|---|---|---|
| 0.01 | 0.22 | 2 | 1 | 0.8 | -1 | 0.2 | 0.3 | 1.2017 | 0.3952 | 4.6550 |
| 0.02 | 0.22 | 2 | 1 | 0.8 | -1 | 0.2 | 0.3 | 0.8486 | 0.4829 | 4.4977 |
| 0.03 | 0.22 | 2 | 1 | 0.8 | -1 | 0.2 | 0.3 | 0.5192 | 0.5598 | 4.3634 |
| 0.01 | 0.23 | 2 | 1 | 0.8 | -1 | 0.2 | 0.3 | -2.6398 | 0.1296 | 4.6178 |
| 0.01 | 0.24 | 2 | 1 | 0.8 | -1 | 0.2 | 0.3 | -6.2069 | -0.1480 | 4.5803 |
| 0.01 | 0.22 | 2.1 | 1 | 0.8 | -1 | 0.2 | 0.3 | -2.2015 | 0.6354 | 4.8951 |
| 0.01 | 0.22 | 2.2 | 1 | 0.8 | -1 | 0.2 | 0.3 | -5.6046 | 0.8756 | 5.1353 |
| 0.01 | 0.22 | 2 | 1.1 | 0.8 | -1 | 0.2 | 0.3 | 8.1282 | -0.0455 | 4.1747 |
| 0.01 | 0.22 | 2 | 1.2 | 0.8 | -1 | 0.2 | 0.3 | 15.0546 | -0.4863 | 3.6945 |
| 0.01 | 0.22 | 2 | 1 | 0.85 | -1 | 0.2 | 0.3 | 6.8968 | -0.2796 | 4.0705 |
| 0.01 | 0.22 | 2 | 1 | 0.9 | -1 | 0.2 | 0.3 | 10.9933 | -0.8632 | 3.5881 |
| 0.01 | 0.22 | 2 | 1 | 0.8 | -1.5 | 0.2 | 0.3 | 3.3604 | -1.9725 | 2.2872 |
| 0.01 | 0.22 | 2 | 1 | 0.8 | -2 | 0.2 | 0.3 | 2.1061 | -2.7285 | 1.5312 |
| 0.01 | 0.22 | 2 | 1 | 0.8 | -1 | 0.3 | 0.3 | 37.0956 | -0.5471 | 3.7126 |
| 0.01 | 0.22 | 2 | 1 | 0.8 | -1 | 0.4 | 0.3 | 72.9896 | -1.4894 | 2.7703 |
| 0.01 | 0.22 | 2 | 1 | 0.8 | -1 | 0.3 | 0.4 | 1.3824 | 0.3225 | 4.3055 |
| 0.01 | 0.22 | 2 | 1 | 0.8 | -1 | 0.3 | 0.5 | 1.5331 | 0.2186 | 4.0566 |

In case of ramped temperature and ramped concentration, Skin friction increases with increase in permeability of porous medium $\kappa$ and Mass Grashof number $Gm$ and otherwise for volume fraction parameter $\emptyset$, Schimdt number $Sc$ and Grashof number $Gr$. If isothermal temperature and constant Surface concentration are considered then skin friction increases with increase in Grashof number $Gr$ and decreases with increase in porous medium $\kappa$, Schimdt number $Sc$,

mass Grashof number $Gm$, volume fraction parameter $\emptyset$ and heat absorption parameter $H$. The increased skin friction is generally a disadvantage in the technical applications.

**Table 4.2:** Nusselt number variation

| $\emptyset$ | $H$ | $t$ | Nusselt number $Nu$ for Ramped Temperature | Nusselt number $Nu$ for isothermal Temperature |
|---|---|---|---|---|
| 0.01 | -1 | 0.3 | 0.7585 | 1.3060 |
| 0.02 | -1 | 0.3 | 0.7436 | 1.2817 |
| 0.03 | -1 | 0.3 | 0.7292 | 1.2580 |
| 0.01 | -1.5 | 0.3 | 0.7647 | 1.3370 |
| 0.01 | -2 | 0.3 | 0.7710 | 1.3678 |
| 0.01 | -1 | 0.3 | 0.7492 | 1.2900 |
| 0.01 | -1 | 0.3 | 0.7403 | 1.2747 |
| 0.01 | -1 | 0.4 | 0.8806 | 1.1489 |
| 0.01 | -1 | 0.5 | 0.9899 | 1.0436 |

**Table 4.3:** Sherwood number variation

| $Sc$ | $Sr$ | $t$ | Sherwood Number $Sh$ for Ramped temperature and ramped concentration | Sherwood Number $Sh$ for isothermal temperature and ramped concentration | Sherwood Number $Sh$ for isothermal temperature and constant Surface concentration. |
|---|---|---|---|---|---|
| 0.22 | 0.2 | 0.3 | -11.8866 | 0.1999 | 0.4047 |
| 0.23 | 0.2 | 0.3 | -11.0634 | 0.2058 | 0.4152 |
| 0.24 | 0.2 | 0.3 | -10.3027 | 0.2116 | 0.4255 |
| 0.22 | 0.3 | 0.3 | -21.4403 | 0.1534 | 0.3582 |
| 0.22 | 0.4 | 0.3 | -30.9940 | 0.1070 | 0.3117 |
| 0.22 | 0.2 | 0.4 | -10.6005 | 0.2437 | 0.3395 |
| 0.22 | 0.2 | 0.5 | -9.7496 | 0.2818 | 0.2941 |

It is evident from Table 4.2 that, Nusselt number Nu decreases on increasing t for ramped temperature and otherwise for isothermal case. It is evident that in either case Nu decreases with increase in volume fraction parameter ∅ and increases with increase in heat absorption parameter. Table 4.3 shows that Sherwood number Sh increases with increase in t or Schimdt number Sc for all thermal cases and otherwise for Soret number Sr for all cases.

## 4.9 Conclusion

Key results can be summarized as follows.

- Nanofluid velocity decreases with increase in volume fraction parameter ∅.
- Nanofluid velocity increases with increase in permeability parameter $\kappa$, Heat generation Parameter $H$ and Soret number $Sr$ while decreases with increase in magnetic parameter $M$.
- Nanofluid velocity is more for isothermal temperature compared to ramped plate.
- Nanofluid temperature is getting accelerated with the progress of volume fraction parameter ∅ and heat generation parameter $H$.
- Concentration increases with increase in Soret number $Sr$.
- Nusselt number $Nu$ decreases on increasing $t$ for ramped temperature and otherwise for isothermal case.
- For isothermal temperature and ramped surface concentration, Skin friction $C_f$ increases with increase in volume fraction parameter ∅.